JMES The International Journal of
Mechanical Engineering and Sciences
https://iptek.its.ac.id/index.php/jmes
e-ISSN 2580-7471

Optimization of Process Parameter in the development of Ecofriendly Brake-pad from Coconut Fruit Fiber (Coir L.) And Oyster Sea Shells (Magallana-Gigas L.)

Eziwhuo S. J.[1*], Ossia C. V.[1], Ojapah M.M.[1]
[1]Department of Mechanical Engineering, University of Port Harcourt, Port Harcourt, Nigeria

Received: 20 March 2023, Revised: 13 February 2024, Accepted: 11 March 2024

Abstract

Coconut Fruit Fiber, CFF, and Oyster Sea Shells, OSS were gathered from the waste peel and suspended in a solution of sodium hydroxide (NaOH) for about 12h in other to eliminate unwanted remnants. Dried CFF and OSS were grounded to powder using an electric grounding machine. Thereafter sieved to 75, 125, and 175μm grain sizes. The based materials, CFF and OSS were prepared into organic-based brake pads by compressive molding with different formulations of base materials, epoxy resin, hardener, graphite friction modifiers, and copper chips. A commercially bought brake pad was used for evaluation in this research. The characterization of the brake pad produced is mostly influenced by molding pressure and grain sizes, respectively. Hence, the density, hardness, tensile strength, and compressive strength values were reduced with a rise in grain sizes. In conclusion, the ideal values of all responses fall within the normal desires of brake pads as they matched positively with commercial lining material. Thus, the characterization of the developed friction lining links suitably and is proficient in creating fewer sounds during the application of braking, owing to its high mechanical properties. Therefore, coconut fruit fibers and oyster sea shells can be a conceivable replacement for asbestos friction brake lining manufacture.

Keywords: Brake pad, Coconut fruit fiber, Oyster sea shell, Grain size, Sample characterization.

1. Introduction

Technology has influenced all human doings. Though one thing is to intensify what technology has prepared, another thing is to enjoy the yielding fruit of technology. It is only when we appreciate the improvement of technology that we can familiarize ourselves with our surroundings and conceivably progress with it. The movement of technology into the forgoing of automobiles gives way to diversified in comfort, and safety, can be better in all the working structures of automobiles, with comparatively easy request and upkeep. In almost all the operating systems of automobiles, the system that needs more consideration in terms of safety while the automobile is in motion is the braking materials Abutu, J. [1] we still need to improve and produce a standard means that can show the situation of brake lining used in the braking method. It has been known that friction lining materials are worn and always replaced when due from time to time. The forward pads will wear more easily than the back pads. Meanwhile, 75 percent of the braking effort comes from the front pads Pravin N. [2].

Factually, in the past Leather and Wood served as brake pad lining materials following the formation of the brake pad materials industry. Nevertheless, their high-temperature production was one reason which caused them to have a partial application that compelled the use of cast iron in 1870 to substitute Leather and Wood Lawal S. [3]. Still cast iron can experience phase alteration leading to the heat furious of a brake disk. The trait of cast iron moved to the introduction of cotton materials as the base material for the production of pads, which permeated the introduction of bitumen solution. However, the a necessity for the working temperature to go beyond the required limit for cotton as based lining materials. High temperatures in the environment constitute the substitution of cotton as based materials with asbestos fibers as based materials. Ibrahim, M. [4], Ibukun Olabisi A. [5], Gabriel, S. A. [6], and Bhaskar, J [7] said that medical research exposed that asbestos can camp in the lungs and prompt hostile respiratory illness. This characteristic of asbestos directed the introduction of other materials but none of them is accurately like asbestos, however, asbestos offered similarities in recital characteristics. In the 1950s, resin-bonded metallic brake lining materials were presented in replacement to asbestos; yet the wear of the disc drum made them to be a weak fit for use. From the 1970s, glass fiber materials were incorporated, but their fragility led to their restricted application while aramid fiber materials,

*Corresponding author. Email: engrsje1985@gmail.com

which were introduced in 1984 as brake lining material, nevertheless were found to have the same relative benefit as asbestos materials but very soft in nature. In 1974, Sepiolite was proposed to substitute asbestos material since it has similarity in property however its constraint is, that it induced pulmonary interstitial fibrosis and inflammation of the lungs. Potassium titanate which was in use linked with a mesothelioma of cancer. The introduction of Ceramic fiber in 1982 as a substitute for asbestos fiber was much more, but Ceramic fiber has a very high brittleness in nature, which necessitated its restricted use.

Materials for friction lining are used in the transmission and braking of different equipment motorcycles, machinery, aircraft, cars, and other automobile applications. The structures of friction lining materials keep on varying to meet the developing technology and necessities of society. Friction lining materials can be classified as organic, metallic, carbon-based, and semi-metallic subject to the conformation of the essential elements. In automobile mechanics, the system is most cases bare to asbestos dust in numerous ways. For automobile devices, such as clutch and brake, dust gathered is always cleaned off before the timeworn pads are replaced using a brush cleaner. Through the application brake pad, airborne can penetrate through the particles of asbestos materials when running. If using old friction linings is seen as difficult to apply, the mechanic man working different of them regularly normalizes the surfaces by using a bench grinder, or the lining will dissolve with oil and dirt inside. Likewise when substituting the brake pads, to increase the engagement process, the mechanic usually grinds the surface pad, drills different rivet holes, and bevels the wheel grinding edges to lower the unwanted noise when applied in motion.

Sometimes, most manufacturers recommend scoring the pad's center with a hacksaw. These processes repeatedly cause the release of some particles of asbestos fiber. The tight link between exposure to asbestos and pulmonary disease was not well known until the mid-1970s. People who have worked on asbestos-inclusion friction materials and workers or supervisors working in the vicinity could have inhaled asbestos fibers while carrying out their duty so placing them in danger of contracting different infections like pericardial mesothelioma, pleural, peritoneal, or cancer of asbestosis (Cueva G. el ta [8], Ahmad Kholil el ta [9], Abutu J [10], Shinde, D [11], and Krishnan el ta [12]).

Mesothelioma is one of these diseases which has a wide latency period, as a result, it can develop at a creeping rate; this can take up to thirty or forty years depending on the initial asbestos exposure. The mesothelioma prognosis for victims of the disease has not been positive as up to date, no cure has been reported for mesothelioma. Hence, different efforts have been made concerning substituting asbestos fibers as friction lining materials. Deshmukh et al [13], Xiao et al [14], and Federici M. S et al [15], reported that metal fibers were applied for addition in the production of brake lining to counter contamination in the ecosystem.

Historically for the past 100 years, asbestos has remained the best in the production of brake pads. The asbestos fibers in the production of brake pads were used as a reinforcement material. This is a result of its good physiomechanical, physical, and chemical properties which persist unaffected in terms of temperature range proficient by brake pads Ahmad Kholil et al [16], Eziwhuo S. J. [17], Obiukwu O. [18], and Achebe CH et al [19]. Hence, due to the danger connected with the management of asbestos, it has lost its applications and as a result of this, eco-friendly materials (Coconut fruit fibers CFF and Oyster sea shell OSS) are being used as replacements for eco-friendly friction lining.

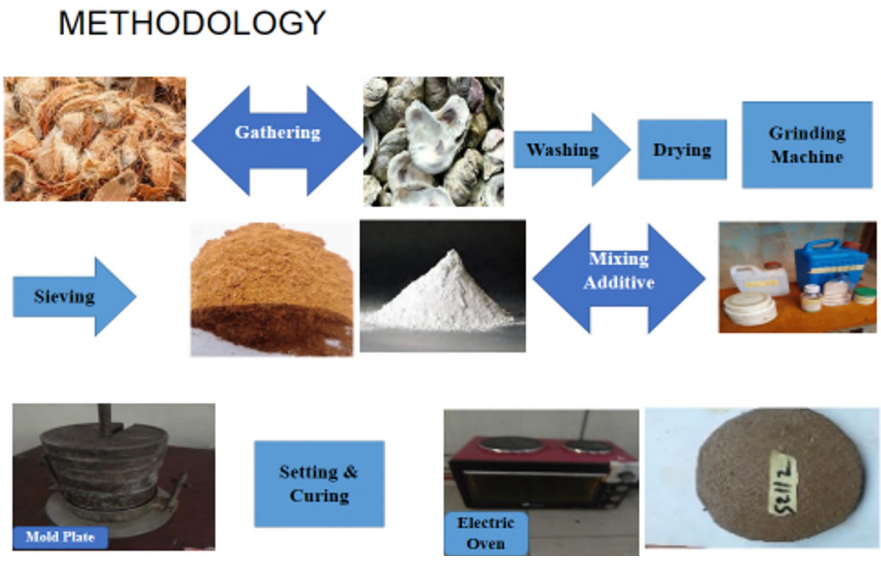

Figure 1. Methodology

(a) Coconut **(b)** Coconut fibers **(c)** Grounded fibers

Figure 2. Coconut Fruit Fiber (*Coir L.*) grounded powder

(a) Oyster sea shell **(b)** grounded powder shell

Figure 3. Oyster Sea Shell (Magallana-Gigas) grounded powder

2. Experimental Methods

2.1. Materials

1. 1. Eco-friendly Materials: (a) Oyster Sea Shell (OSS) (Magallana-Gigas L) (Reinforcement), (b) Coconut Fruit Fiber (CFF) (Coir L) (Reinforcement)
2. 1. Additive: (a) Copper Oxide (Abrasive), (b) Graphite (Friction Modifier or Solid Lubricant), (c) Epoxy Resin (Binder), (d) Hardener (Catalyst).

2.2. Preparation of Coconut Fruit Fiber (CFF)

Coconut Fruit Fiber (CFF) which were brought from the waste peel of coconut fruit fibers. Collected in Engr. Second Justice Eziwhuo Compound, Rumuche Emohua Rives State Nigeria, and deferred in a mixture of sodium hydroxide (NaOH) for twelve hours to eradicate unwanted remnants. The fibers as shown in Figure 2. were washed with clean water to confiscate the solution (sodium hydroxide) and dehydrated in the hot environment for about five days. The dried CFF was grounded into powder using an electric grounding machine found at the Civil Engineering Laboratory, University of Port Harcourt, Port Harcourt Rivers State Nigeria. Thereafter sieved using a mesh size of 75 μm, 125 μm, and 175 μm aperture found at Civil Engineering Laboratory, University of Port Harcourt, Port-Harcourt Rivers State Nigeria.

2.3. Preparation of Oyster Sea Shell (OSS)

Oyster Sea Shells (OSS) were collected in the dustbin riverbank at Rumuche Emohua, Rivers State Nigeria. The Oyster Sea Shells OSS as shown in Figure 3. are washed with distilled water in other to eliminate unwanted and therefore dried in the sun for eight hours. The dried OSS was ground into powder using an electric crushing machine found at the Engineering Laboratory, University of Port Harcourt Rivers State. Thereafter sieved using a mesh size of 75 μm, 125 μm, and 175 μm aperture found at Civil Laboratory, University of Port Harcourt, Nigeria.

2.4. Graphite Powder (Friction modifier)

The graphite powder as shown in Figure 4(b), severed as friction in terms of changing. Friction transformers reduce friction coefficient, due to their low fuel intake. For most friction modifiers, the crystal structure consists of layers called molecular platelets, which effortlessly move over each other when applied. The friction modifiers used in this report were Solid lubricants and were obtained from used 1.5-volt batteries. The 1.5 volts used batteries were prepared by removing the graphite rod from the used batteries, washing the graphite rods using soap and detergent, drying them in the sun for 24 hours, crushing the dried rod using mortar and pestles; grinding using a grinder machine with sieving using a mesh size aperture of 75 μm.

2.5. Copper Powder (Abrasive)

In preparing these copper powders as shown in Figure 5, 20mm copper rod and hand-filler were bought in the Mile-3 market, Rivers State Nigeria. Hand filler was used to cut in the surface of the copper rod, and copper powder was formed which served as an abrasive.

(a) **(b)**

Figure 4. (a) Tiger head batteries (b) Graphite powder

Figure 5. Copper powder

Table 1. Composition of Brake-Bad Sample

REINFORCEMENT	Sample M1(g)	Sample M2(g)	Sample M3(g)
CFF	0	27	54
OSS	54	27	0
EPOXY	30	30	30
HARDENER	15	15	15
COPPER	0.5	0.5	0.5
GRAPHITE	0.5	0.5	0.5
TOTAL	100	100	100

2.6. Formulation of Different Based Samples

The based materials, Coconut Fruit Fiber (CFF), and Oyster Sea Shell (OSS) were prepared into the molding of Brake- pad with different additives added. Three dissimilar formulations which are: M1, M2, and M3 were prepared by changing the coconut fruit fiber with oyster sea shell substances (Table 1, 2, 3). Coconut fruit fiber powder and Oyster Sea shell dust were the basic materials, hardener epoxy resin was the binder materials, graphite was the friction modifier, and copper chips were used as abrasive materials that boost the thermal conductivity. The control brake pads were bought in the market for evaluation. Ensuing for each of the succeeding samples required, coconut fruit fiber powder, oyster sea shell powder, graphite powder, and copper chips were mixed comprehensively till a uniform combination was formed for the required usage. Mixing of catalyst (hardener and epoxy) in a proportion of 2:1. All the friction lining materials were blended to give an upswing paplike combination. The above-combined combination was conveyed into an already preserved steel molding plate. The mixture was allowed two minutes to stay by which forming took place which is an exothermic reaction as the molding surface became hot. At this juncture, variations of pressures were realistic and given 3 hours upon which complete preserving was engaged and immediately transferred to an electric oven with variations of molding temperature and heat treatment time.

2.7. Characterization of samples

Developed samples were tested to evaluate the Density, Compressive strength, Ultimate tensile strength, and Brinel Hardness. These tests were characterized using standard testing processes as well as machine specifications.

2.7.1. Density

$$Density(D) = \frac{M}{V} = \frac{M}{V_2 - V_1} \tag{1}$$

Where M = Mass of the Sample, V = Sample Volume

The mass samples were obtained using a weighing electric machine seen in Figure 1. which has an accuracy of ±0.01.

The volume of the samples: Sample volumes were analyzed using the fluid displacement technique.A conical flask of 1000cL filled with water to the middle and tabulated, V1. The developed samples were inserted in the already filled water, V1, and read V2. This procedure was used repeatedly for all the samples. Where the results for calculated sample density are shown see Table 4.

2.7.2. Brinel Hardness test

Brinell hardness was experimented with by using an Avery hardness testing machine (Made in England capacity: 120kg, type: 6406, number: E65226, REQU NO: 5/07U1/1, Indent NO: 454/64-65). The test was conducted by using the loading force (P) of 40kgf and was conceded with these stipulations given customary ASTM D2240 type D scale. The hardness test was analyzed through the diameter of indentation (d) and the indenter (D) below the weight. The hardness numbers of the three experimental tests in each of the brake pad samples were noted and the average mean was considered using equation 2. Mathematically: Brinell hardness number, BHN

$$BHN = \frac{2P}{\pi D(D - \sqrt{D^2 - d^2})} \tag{2}$$

Table 2. Four factors and process parameters of three levels

Factors	Lower Levels (-1)	Middle Levels (0)	Upper Levels (+1)
Reinforcement Material (RM)	M1 (0 CFF /100 OSS)	M2 (50 CFF /50 OSS)	M3 (100 CFF /0 OSS)
Moulding Pressure, Pm (KPa)	9.93	11.25	12.57
Moulding Temperature, T_m(^{o}C)	120	150	180
Heat Treatment Time, $T_h t$ (min)	60	120	180

Table 3. The experimental layout of RSM- Box – Behnken Design BBD (Four Factors and Three Levels)

RUNS	Reinforcement Material	P_m (Pa)	T_m(^{o}C)	T_{ht} (minute)
1	M1	9.93	150	120
2	M3	9.93	150	120
3	M1	12.57	150	120
4	M3	12.57	150	120
5	M2	11.25	120	60
6	M2	11.25	180	60
7	M2	11.25	120	180
8	M2	11.25	180	180
9	M1	11.25	150	60
10	M3	11.25	150	60
11	M1	11.25	150	180
12	M3	11.25	150	180
13	M2	9.93	120	120
14	M2	12.57	120	120
15	M2	9.93	180	120
16	M2	12.57	180	120
17	M1	11.25	180	120
18	M3	11.25	120	120
19	M1	11.25	180	120
20	M3	11.25	180	120
21	M2	9.93	150	60
22	M2	12.57	150	60
23	M2	9.93	150	80
24	M2	12.57	150	80
25	M2	11.25	150	120
26	M2	11.25	150	120
27	M2	11.25	150	120

2.7.3. Compressive and Tensile Strength

Compressive strength test was accomplished with ASTM D695 using a 40KN testing machine that has specifications made in the UK, Type 'W', serial No 10975. Thus, the brake pad samples were placed in-between the surface of the compression tool and it was confirmed that the line center of every specimen was in line with the plunger center line. The surface of the compression tool is parallel to the ends of the cubic-shaped specimen dimensioned as 20 x 20 x 5mm. The compression tool plunger touches the crosshead of the testing machine through adjustment. Each test brake pad sample was subjected to a compressive strength force while gradually loading it before failure occurred. The three samples of brake pads were tested for each specimen were loads at which failure occurred and deflections shown on the output display unit of the machine all was documented. The average mean value for all the experimental results in this report was considered for each sample test. Compressive strength analysis, tensile strength, and the whole surface area of the sample were analyzed from equation 3, 4, and 5 respectively.

$$Compressive\,strength = \frac{maximum\,force\,break, F}{total\,surface\,area, A} \quad (3)$$

$$Ultimate\,tensile\,strength\,UTS = \frac{maximum\,load, l}{cross\,sectional\,area, a} \quad (4)$$

$$Total\,surface\,area, A = 2(L_h + L_w + w_h) \quad (5)$$

Where L is the length of the samples, h is the height of the samples, and w is the width of the samples respectively.

3. Results and Discussions

3.1. Experimental results

Table 4. below, shows the results of the physio-mechanical properties performed with the developed brake lining samples with the commercial asbestos brake pad with the model: ICER 140403-700 which were used for evaluation to compare with the newly developed organic brake pad specimens and variation of particle sizes.

3.2. The Regression Equation of Density is

$$\begin{aligned} Density\,(g/cm^3) = 3.381 - 0.06758X_1 - 0.08475X_2 + \\ 0.1025X_3 + 0.045167X_4 - 0.144X_1X_2 + 0.035X_1X_3 + \\ 0.04775X_1X_4 + 0.0385X_2X_3 + 0.005125X_2X_4 - \\ 0.175X_3X_4 + 0.010958X_1^2 - 0.04329X_2^2 + \\ 0.014083X_3^2 - 0.23892X_4^2 \end{aligned} \quad (6)$$

When X_3 and X_4 = 0

$$\begin{aligned} Density(g/cm^3) = 3.381 - 0.06758X_1 - 0.08475X_2 \\ -0.144X_1X_2 + 0.010958X_1^2 - 0.04329X_2^2 \end{aligned} \quad (7)$$

Table 4. Experimental Responses (Density, Hardness, Compression, Tensile strength)

SAMPLES	**Density (g/cm^3)**	**Brinell Hardness Number (BHN)**	**Compressive Strength (Mpa)**	**Ultimate Tensile Strength (Mpa)**
S1122	3.266	49.92	2.5	3.33
S3122	3.512	47.79	2.41	2.98
S1322	3.473	55.6	2.09	3.15
S3322	3.019	52.79	1.98	1.98
S2211	2.94	49.14	2.46	4.5
S2231	3.258	54.02	2.32	4.09
S2213	3.402	51.98	2.19	3.93
S2233	3.024	48.05	2.49	2.19
S1221	3.209	53.36	1.99	1.99
S3221	3,020	55.19	2.5	2.47
S1223	3.293	47.07	2.49	3.48
S3223	3.295	47.46	1.89	3.24
S2112	3.383	54.99	2.53	2.51
S2312	3.11	50	2.59	4.17
S2132	3.619	51.93	2.54	4.5
S2332	3.5	48.11	2.49	2.5
S1212	3.297	55.66	2.6	2.93
S3212	3.081	49.09	2.61	2.12
S1232	3.559	53.16	1.92	2.65
S3232	3.483	52.91	2.78	3.92
S2121	3.164	51.22	2.64	3.77
S2321	2.954	54.75	2.7	4.1
S2123	3.039	47.03	1.92	2.43
S2323	3.034	48.08	2.49	4.42
S2222	3.381	48.99	2.5	3.95
S2222	3.381	48.99	2.5	3.95
S2222	3.381	48.99	2.5	3.95
CBP	3.199	53.5	2.48	3.15

$$F(z) = 3.381 - 0.06758 * ((x-50)/50) - 0.08475* ((y-11.25)/1.32) - 0.144 * ((x-50)/50)* ((y-11.25)/1.32) + 0.010958 * ((x-50)/5)^2 -0.04329 * ((y-11.25)/1.32)^2 \quad (8)$$

Figure 6. shows the density difference concerning the molding pressure and size of grain, indicating that density increases with reductions in the size of grain and molding pressure. The influence of the density and molding pressure on grain size implies that a decrease in grain size adds more optimization processes in the automobile industry. Commercial brake pad (CBP) has a density of 3.199g/cm3 which implies that the CBP density is lighter than produced samples brake pad. Has a tendency of mechanical failure when the stresses are induced by external forces. The produced samples are more reliable to continue to function as expected for a specific duration within a specified environment.

3.3. The Regression Equation of Brinel Hardness is

$$B.H.Eq. = 47.34667 - 0.735X_1 + 1.208333X_2 -1.19833X_3 - 2.08167X_4 + 1.1025X_1X_2 + 0.1725X_1X_3 -0.54X_1X_4 + 0.23X_2X_3 - 1.9125X_2X_4 - 2.2025X_3X_4 +3.995833X_1^2 + 1.265833X_2^2 + 3.360833X_3^2 - 0.09917X_4^2 \quad (9)$$

When X_3 and X_4 = 0

$$B.H.Eq. = 47.34667 - 0.735X_1 + 1.208333X_2 +1.1025X_1X_2 + 3.995833X_1^2 + 1.265833X_2^2 \quad (10)$$

$$F(x) = 47.34667 - 0.735 * ((x-50)/50) +1.208333 * ((y-11.25)/1.32) + 1.1025* ((x-50)/50) * ((y-11.25)/1.32) + 3.995833* ((x-50)/50)^2 + 1.265833 * ((y-11.25)/1.32)^2 \quad (11)$$

In the 3-D surface plot shown in Figure 7, hardness varies with molding pressure and size of grain. Grain size decreases with an increase in molding pressure and Brinell Hardness Number (BHN). It can be observed from the 3-D surface plot that the highest hardness of the developed samples 54BHN was superior to the hardness of the commercially bought brake pad (53.50BHN), which caused the growth in surface particle area that resulted from improvement in bonding and Epoxy resin. Therefore, produced brake pads will be more reliable than commercial brake pads in terms of mechanical failure. According to the theory of Holm's wear, that said wear rate increases while hardness decreases through the lenient surface of a coupling pair B. Bhushan [20].

3.4. Regression equation of Compressive strength is

$$CSeq.(Mpa) = 2.5 + 0.065x_1 - 0.14417x_2 +0.145x_1x_2 + 0.000833x_1^2 \smile 0.017083x_2^2 \quad (12)$$

$$F(x) = 2.5 + 0.065 * ((x-50)/50) - 0.14417 ((y-11.25)/1.32) + 0.145 * ((x-50)/50)* ((y-11.25)/1.32) + 0.000833 * ((x-50)/50)^2 +0.017083 * ((y-11.25)/1.32)^2 \quad (13)$$

Figure 8. Shown 3D surface plot of particle size and molding pressure on the compressive strength variation. The brake pad samples produced increased with a decrease in particle sizes, and are likely to be dependent on the hardness of grain sizes. The reductions in particle size brought about the reduction of mechanical failure in nucleation sites and increased strength of interfacial closeness. Hence, from the lower compressive loads, the brake pad samples with larger grain sizes fail owing to the collective influence of feebler ties, transmission sites, and more crack instigation, as reported by Ossia C.V. et [21,22]. From the graph, the highest compressive strength of the developed brake pad was 2.58Mpa greater than that of commercial brake pad 2.48Mpa; which implies low wear and tears in the brake pad produced and capable of withstanding mechanical failure than commercial brake pad. The produced samples are more reliable to continue to function as expected for a specific duration within a specified environment. From this research, it was observed that the relationship between grain size particles and compressive strength is in line with Yawas, D.S el ta [13], and Jaya H el ta [14].

3.5. Regression equation of Ultimate tensile strength is

$$UTS\,eq.(Mpa) = 3.963333 - 0.48333x_1 +0.181667x_2 + 0.35x_1x_2 - 0.80917x_1^2 \smile 0.21167x_2^2 \quad (14)$$

$$F(x) = 3.963333 - 0.48333 * ((x-50)/50) +0.181667 * ((y-11.25)/1.32) + 0.35* ((x-50)/50) * ((y-11.25)/1.32) - 0.80917* ((x-50)/50)^2 - 0.21167 * ((y-11.25)/1.32)^2 \quad (15)$$

Figure 9. 3-D surface plot showing the outcome of molding pressure and grain size on UTS The 3-D surface plot shown in Figure 9. designates alteration in two significant aspects (the most substantial) touches the properties of oyster sea shells and coconut fruit fiber which served as reinforcement in brake pad production.

Table 5. Density Regression Analysis

Regression Statistics	
Multiple R	0.957039
R Square	0.915924
Adjusted R Square	0.781402
Standard Error	0.094704
Observations	27

ANOVA

	df	*SS*	*MS*	*F*	*Significance F*
Regression	16	0.977072	0.061067	6.808725	0.002008
Residual	10	0.089689	0.008969		
Total	26	1.066762			

	Coefficients	*Standard Error*	*t Stat*	*P-value*	*Lower 95%*	*Upper 95%*	*Lower 95.0%*	*Upper 95.0%*
Intercept	3.381	0.054678	61.83514	2.98E-14	3.259171	3.502829	3.259171	3.502829
X Variable 1	-0.06758	0.027339	-2.47206	0.032988	-0.1285	-0.00667	-0.1285	-0.00667
X Variable 2	-0.08475	0.027339	-3.09999	0.011251	-0.14566	-0.02384	-0.14566	-0.02384
X Variable 3	0.1025	0.027339	3.749247	0.003789	0.041585	0.163415	0.041585	0.163415
X Variable 4	0.045167	0.027339	1.652107	0.129521	-0.01575	0.106081	-0.01575	0.106081
X Variable 5	-0.144	0.047352	-3.04104	0.01244	-0.24951	-0.03849	-0.24951	-0.03849
X Variable 6	0.035	0.047352	0.739141	0.476812	-0.07051	0.140507	-0.07051	0.140507
X Variable 7	0.04775	0.047352	1.0084	0.337039	-0.05776	0.153257	-0.05776	0.153257
X Variable 8	0.0385	0.047352	0.813056	0.435116	-0.06701	0.144007	-0.06701	0.144007
X Variable 9	0.05125	0.047352	1.082314	0.30452	-0.05426	0.156757	-0.05426	0.156757
X Variable 10	-0.174	0.047352	-3.67459	0.004285	-0.27951	-0.06849	-0.27951	-0.06849
X Variable 11	0	0	65535	#NUM!	0	0	0	0
X Variable 12	0	0	65535	#NUM!	0	0	0	0
X Variable 13	0.010958	0.041008	0.267223	#NUM!	-0.08041	0.10233	-0.08041	0.10233
X Variable 14	-0.04329	0.041008	-1.05568	0.31595	-0.13466	0.04808	-0.13466	0.04808
X Variable 15	0.014083	0.041008	0.343427	0.738388	-0.07729	0.105455	-0.07729	0.105455
X Variable 16	-0.23892	0.041008	-5.82607	0.000167	-0.33029	-0.14754	-0.33029	-0.14754

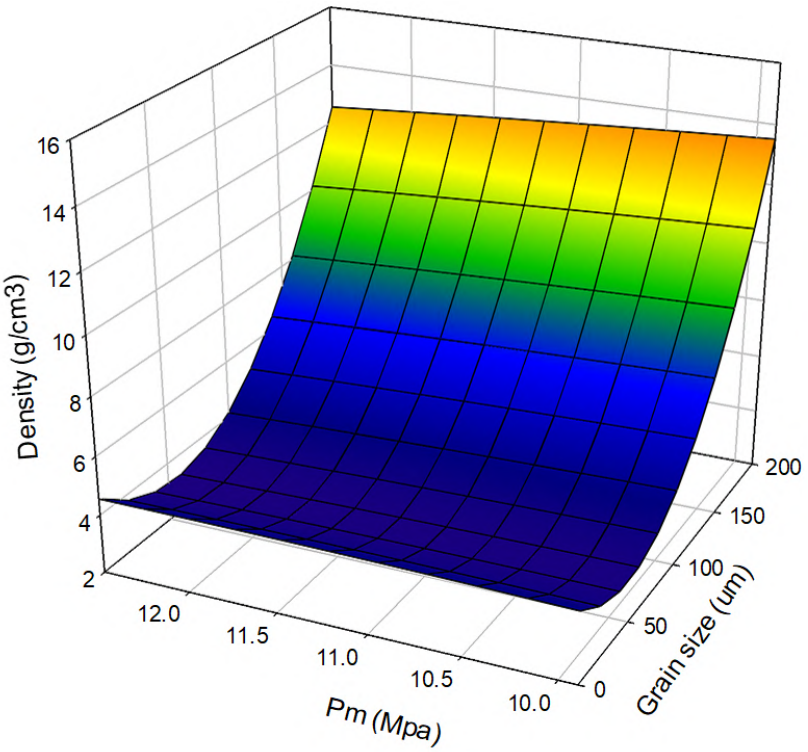

Figure 6. Surface plot of 3D showing the influence of molding pressure and grain size in density

Table 6. Brinell Hardness Regression Analysis

Regression Statistics	
Multiple R	0.959537
R Square	0.920712
Adjusted R Square	0.793851
Standard Error	1.673901
Observations	27

ANOVA

	df	SS	MS	F	Significance F
Regression	16	325.3676	20.33548	7.25763	0.001543
Residual	10	28.01945	2.801945		
Total	26	353.3871			

	Coefficients	*Standard Error*	*t Stat*	*P-value*	*Lower 95%*	*Upper 95%*	*Lower 95.0%*	*Upper 95.0%*
Intercept	47.34667	0.966427	48.99145	3.03E-13	45.19333	49.5	45.19333	49.5
X Variable 1	-0.735	0.483214	-1.52107	0.159213	-1.81167	0.341667	-1.81167	0.341667
X Variable 2	1.208333	0.483214	2.500619	0.031413	0.131666	2.285	0.131666	2.285
X Variable 3	-1.19833	0.483214	-2.47992	0.032547	-2.275	-0.12167	-2.275	-0.12167
X Variable 4	-2.08167	0.483214	-4.30796	0.001542	-3.15833	-1.005	-3.15833	-1.005
X Variable 5	1.1025	0.836951	1.317282	0.217128	-0.76234	2.967342	-0.76234	2.967342
X Variable 6	0.1725	0.836951	0.206105	0.840844	-1.69234	2.037342	-1.69234	2.037342
X Variable 7	-0.54	0.836951	-0.6452	0.533321	-2.40484	1.324842	-2.40484	1.324842
X Variable 8	0.23	0.836951	0.274807	0.789058	-1.63484	2.094842	-1.63484	2.094842
X Variable 9	-1.9125	0.836951	-2.28508	0.045392	-3.77734	-0.04766	-3.77734	-0.04766
X Variable 10	-2.2025	0.836951	-2.63158	0.025094	-4.06734	-0.33766	-4.06734	-0.33766
X Variable 11	0	0	65535	#NUM!	0	0	0	0
X Variable 12	0	0	65535	#NUM!	0	0	0	0
X Variable 13	3.995833	0.72482	5.51286	#NUM!	2.380833	5.610834	2.380833	5.610834
X Variable 14	1.265833	0.72482	1.74641	0.111325	-0.34917	2.880834	-0.34917	2.880834
X Variable 15	3.360833	0.72482	4.636781	0.000927	1.745833	4.975834	1.745833	4.975834
X Variable 16	-0.09917	0.72482	-0.13682	0.893892	-1.71417	1.515834	-1.71417	1.515834

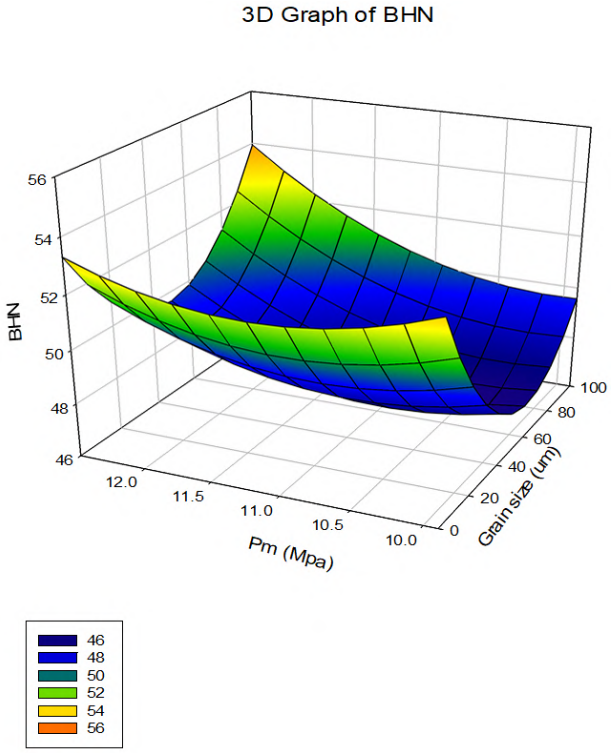

Figure 7. 3-D surface plot displaying the result of the molding pressure and grain size on hardness

Table 7. Compressive Strength Regression Analysis

Regression Statistics	
Multiple R	0.96766
R Square	0.936366
Adjusted R Square	0.83455
Standard Error	0.122714
Observations	27

ANOVA

	df	SS	MS	F	Significance F
Regression	16	2.215843	0.13849	9.19672	0.000565
Residual	10	0.150587	0.015059		
Total	26	2.36643			

	Coefficients	*Standard Error*	*t Stat*	*P-value*	*Lower 95%*	*Upper 95%*	*Lower 95.0%*	*Upper 95.0%*
Intercept	2.5	0.070849	35.28642	7.93E-12	2.342139	2.657861	2.342139	2.657861
X Variable 1	0.065	0.035424	1.834894	0.096401	-0.01393	0.14393	-0.01393	0.14393
X Variable 2	-0.14417	0.035424	-4.0697	0.002251	-0.2231	-0.06524	-0.2231	-0.06524
X Variable 3	0.059167	0.035424	1.670224	0.12583	-0.01976	0.138097	-0.01976	0.138097
X Variable 4	-0.03167	0.035424	-0.89392	0.392369	-0.1106	0.047264	-0.1106	0.047264
X Variable 5	0.145	0.061357	2.363224	0.039734	0.008288	0.281712	0.008288	0.281712
X Variable 6	0.2775	0.061357	4.522723	0.001104	0.140788	0.414212	0.140788	0.414212
X Variable 7	0.0325	0.061357	0.529688	0.607886	-0.10421	0.169212	-0.10421	0.169212
X Variable 8	-0.1975	0.061357	-3.21887	0.009193	-0.33421	-0.06079	-0.33421	-0.06079
X Variable 9	-0.235	0.061357	-3.83005	0.003319	-0.37171	-0.09829	-0.37171	-0.09829
X Variable 10	-0.0725	0.061357	-1.18161	0.264697	-0.20921	0.064212	-0.20921	0.064212
X Variable 11	0	0	65535	#NUM!	0	0	0	0
X Variable 12	0	0	65535	#NUM!	0	0	0	0
X Variable 13	0.000833	0.053137	0.015683	#NUM!	-0.11756	0.119229	-0.11756	0.119229
X Variable 14	0.017083	0.053137	0.321499	0.754452	-0.10131	0.135479	-0.10131	0.135479
X Variable 15	0.167083	0.053137	3.144412	0.010432	0.048688	0.285479	0.048688	0.285479
X Variable 16	0.003333	0.053137	0.062731	0.951217	-0.11506	0.121729	-0.11506	0.121729

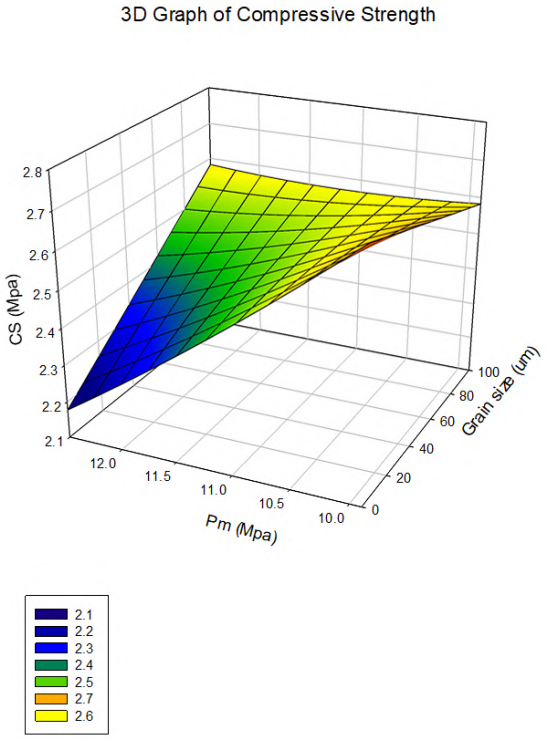

Figure 8. 3D surface plot viewing the result of molding pressure and grain size on comprehensive strength

Table 8. Ultimate Tensile Strength Regression Analysis

Regression Statistics	
Multiple R	0.965553
R Square	0.932292
Adjusted R Square	0.823958
Standard Error	0.380386
Observations	27

ANOVA

	df	SS	MS	F	Significance F
Regression	16	19.9232	1.2452	8.605773	0.000752
Residual	10	1.446936	0.144694		
Total	26	21.37014			

	Coefficients	*Standard Error*	*t Stat*	*P-value*	*Lower 95%*	*Upper 95%*	*Lower 95.0%*	*Upper 95.0%*
Intercept	3.963333	0.219616	18.04665	5.85E-09	3.473998	4.452668	3.473998	4.452668
X Variable 1	-0.48333	0.109808	-4.40162	0.001332	-0.728	-0.23867	-0.728	-0.23867
X Variable 2	0.181667	0.109808	1.654403	0.129048	-0.063	0.426334	-0.063	0.426334
X Variable 3	-0.405	0.109808	-3.68826	0.004189	-0.64967	-0.16033	-0.64967	-0.16033
X Variable 4	-0.17833	0.109808	-1.62405	0.135429	-0.423	0.066334	-0.423	0.066334
X Variable 5	0.35	0.190193	1.840235	0.095562	-0.07378	0.773777	-0.07378	0.773777
X Variable 6	0.605	0.190193	3.180978	0.009803	0.181223	1.028777	0.181223	1.028777
X Variable 7	0.47	0.190193	2.471173	0.033038	0.046223	0.893777	0.046223	0.893777
X Variable 8	-0.96	0.190193	-5.0475	0.000501	-1.38378	-0.53622	-1.38378	-0.53622
X Variable 9	0.16	0.190193	0.84125	0.419869	-0.26378	0.583777	-0.26378	0.583777
X Variable 10	-0.46	0.190193	-2.4186	0.036148	-0.88378	-0.03622	-0.88378	-0.03622
X Variable 11	0	0	65535	#NUM!	0	0	0	0
X Variable 12	0	0	65535	#NUM!	0	0	0	0
X Variable 13	-0.80917	0.164712	-4.91261	#NUM!	-1.17617	-0.44217	-1.17617	-0.44217
X Variable 14	-0.21167	0.164712	-1.28507	0.227733	-0.57867	0.155335	-0.57867	0.155335
X Variable 15	-0.42167	0.164712	-2.56002	0.028372	-0.78867	-0.05467	-0.78867	-0.05467
X Variable 16	0.245833	0.164712	1.492504	0.166428	-0.12117	0.612835	-0.12117	0.612835

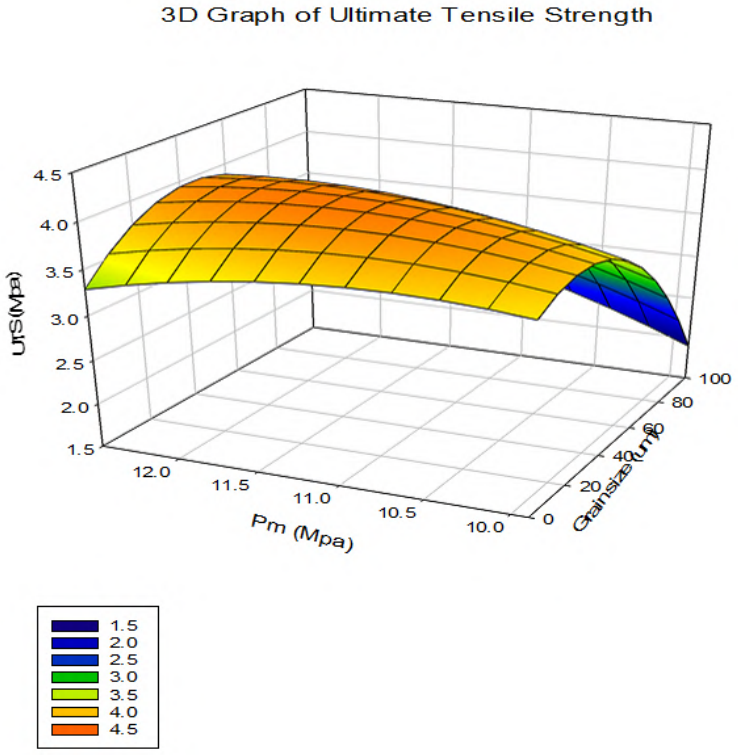

Figure 9. 3-D surface plot showing the outcome of molding pressure and grain size on UTS

4. Conclusions

In the present research, the use of Coconut fruit fibers and Oyster Sea shells as reinforcement materials for the manufacturing of organic brake lining. The recently framed organic brake pads were considered by examining the characterization (physio-mechanical properties). With all the results achieved experiment, the following decisions can be pinched: The characterization of the developed organic brake pad varies, as the four process factors amalgamation (Reinforcement materials RM, Molding PressureP_m, Molding TemperatureT_m, and Heat treatment TimeT_{ht}) change. From the outcome, the brake pad samples produced with diverse process influences change the performance values in the processes. From this experiment, the best parameter for coconut fruit fiber and oyster sea shell-reinforcement friction lining composite would be produced by using molding pressureP_ms (12.57Mpa, 11.25Mpa, 9.93Mpa); molding temperatureT_m (180^{o}C, 150^{o}C, 120^{o}C), and heat treatment timeT_{ht}s (180 min, 120 min, 60 min) respectively. The characterization of the brake pad produced is mostly influenced by molding pressure and grain sizes, respectively. Hence the hardness, density, compressive strength, and tensile strength test values increase with a decrease in the size of grain. Therefore, the best values for these responses are within the normal expectations of brake pads as friction lining which compared positively with the commercial asbestos brake pads. Thus from the research, it can be summarized that the characterization of developed organic materials for brake pads matches acceptably and it can be proficient in generating low noise and weak vibration in the process of brake performance because of its extraordinary efficacy in terms of mechanical properties. Therefore, coconut fruit fibers and oyster sea shell materials can be aid as a conceivable replica for asbestos materials in terms of brake pad production.

Acknowledgment

The authors thank the Department of Mechanical and Civil Engineering Laboratory, University of Port-Harcourt, Nigeria for using their Lab. for this experiment. Also acknowledge Mechanical Engineering Workshop, Federal Polytechnic Kaduna, Kaduna State Nigeria.

References

[1] J. Abutu, S. A. Lawal, M. Ndaliman, R. Lafia-Araga, O. Adedipe, and I. Choudhury, "Production and characterization of brake pad developed from coconut shell reinforcement material using central composite design," *SN Applied sciences*, vol. 1, pp. 1–16, 2019.

[2] P. Jawarikar, S. Khan, and B. Kshirsagar, "Structural optimization, thermal and vibration analysis of two wheeler disc brake rotor," *Int J Innovative Res Sci Eng*, vol. 2, no. 8, pp. 169–186, 2016.

[3] S. S. Lawal, K. C. Bala, and A. T. Alegbede, "Development and production of brake pad from sawdust composite," 2017.

[4] I. Mutlu *et al.*, "Investigation of tribological properties of brake pads by using rice straw and rice husk dust.," *Journal of Applied sciences*, vol. 9, no. 2, pp. 377–381, 2009.

[5] A. I. Olabisi, A. N. Adam, and O. M. Okechukwu, "Development and assessment of composite brake pad using pulverized cocoa beans shells filler," *International Journal of Materials Science and Applications*, vol. 5, no. 2, pp. 66–78, 2016.

[6] G. S.A., "Development of automobile disk brake pads using eco-friendly periwinkle shell and fan palm shell materials," *PhD thesis*, pp. 1–145, 2016.

[7] V. Singh and J. Bhaskar, "Physical and mechanical properties of coconut shell particles reinforcedepoxy composite," *J Mat. Environ. Sci*, vol. 4, pp. 227–232, 2013.

[8] G. Cueva, A. Sinatora, W. L. Guesser, and A. P. Tschiptschin, "Wear resistance of cast irons used in brake disc rotors," *Wear*, vol. 255, no. 7-12, pp. 1256–1260, 2003.

[9] A. Kholil, S. T. Dwiyati, J. P. Siregar, and R. Sulaiman, "Development brake pad from composites of coconut fiber, wood powder and cow bone for electric motorcycle," *Int. J. Sci. Technol. Res*, vol. 9, pp. 2938–2942, 2020.

[10] J. Abutu, S. A. Lawal, M. B. Ndaliman, R. A. Lafia-Araga, O. Adedipe, and I. A. Choudhury, "Effects of process parameters on the properties of brake pad developed from seashell as reinforcement material using grey relational analysis," *Engineering science and technology, an international journal*, vol. 21, no. 4, pp. 787–797, 2018.

[11] D. Shinde and K. Mistry, "Asbestos base and asbestos free brake lining materials: comparative study," *World Scientific News*, vol. 61, no. 2, pp. 192–198, 2017.

[12] G. S. Krishnan, L. G. Babu, R. Pradhan, and S. Kumar, "Study on tribological properties of palm kernel fiber for brake pad applications," *Materials Research Express*, vol. 7, no. 1, p. 015102, 2019.

[13] H. P. Deshmukh and N. K. Patil, "Experimentation and analysis of three different compositions of semi-metallic brake pads for wear rate under dry friction condition," *International Journal of Engineering Research & Technology (IJERT)*, vol. 4, no. 10, 2015.

[14] X. Xiao, Y. Yin, J. Bao, L. Lu, and X. Feng, "Review on the friction and wear of brake materials,"

Advances in Mechanical Engineering, vol. 8, no. 5, p. 1687814016647300, 2016.

[15] M. Federici, S. Gialanella, M. Leonardi, G. Perricone, and G. Straffelini, "A preliminary investigation on the use of the pin-on-disc test to simulate off-brake friction and wear characteristics of friction materials," *Wear*, vol. 410, pp. 202–209, 2018.

[16] A. Kholil, S. Dwiyati, A. Sugiharto, and I. Sugita, "Characteristics composite of wood powder, coconut fiber and green mussel shell for electric motorcycle brake pads," in *Journal of Physics: Conference Series*, vol. 1402, p. 055095, IOP Publishing, 2019.

[17] S. Eziwhuo and T. Joseph, "Performance evaluation of non-edible vegetable seed oil as cutting fluid in metal turning operation," *World Journal of Engineering Research and Technology (WJERT)*, vol. 6, no. 4, pp. 354–366, 2020.

[18] O. Obiukwu, I. Opara, and H. Udeani, "Study on the mechanical properties of palm kernel fibre reinforced epoxy and poly-vinyl alcohol (pva) composite material," *International Journal of Engineering and Technologies*, vol. 7, pp. 68–77, 2016.

[19] C. Achebe, E. Obika, J. Chukwuneke, and O. Ani, "Optimisation of hybridised cane wood–palm fruit fibre frictional material," *Proceedings of the Institution of Mechanical Engineers, Part L: Journal of Materials: Design and Applications*, vol. 233, no. 12, pp. 2490–2497, 2019.

[20] B. Bhushan, *Principles and applications of tribology*. John Wiley & Sons, 1999.

[21] C. Ossia, A. Big-Alabo, and E. Ekpruke, "Effect of grain size on the physicomechanical properties," *Advances in Manufacturing Science and Technology*, vol. 44, no. 4, pp. 135–144, 2020.

[22] C. V. Ossia and A. Big-Alabo, "Development and characterization of green automotive brake pads from waste shells of giant african snail (achatina achatina l.)," *The International Journal of Advanced Manufacturing Technology*, vol. 114, pp. 2887–2897, 2021.

[23] D. Yawas, S. Aku, and S. Amaren, "Morphology and properties of periwinkle shell asbestos-free brake pad," *Journal of King Saud University-Engineering Sciences*, vol. 28, no. 1, pp. 103–109, 2016.

[24] H. Jaya, M. F. Omar, H. M. Akil, Z. A. Ahmad, and N. N. Zulkepli, "Effect of particle size on mechanical properties of sawdust-high density polyethylene composites under various strain rates," *BioResources*, vol. 11, no. 3, pp. 6489–6504, 2016.